ACS APPLIED MATERIALS & INTERFACES

Research Article

www.acsami.org

Alkaline Post-Treatment of Cd(II)−Glutathione Coordination Polymers: Toward Green Synthesis of Water-Soluble and Cytocompatible CdS Quantum Dots with Tunable Optical Properties

Pengcheng Huang, Qin Jiang, Ping Yu, Lifen Yang,* and Lanqun Mao*

Beijing National Laboratory for Molecular Sciences, Key Laboratory of Analytical Chemistry for Living Biosystems, Institute of Chemistry, Chinese Academy of Sciences, Beijing 100190, China

Supporting Information

ABSTRACT: In this study, we demonstrate a facile and environmentally friendly method for the synthesis of glutathione (GSH)-capped water-soluble CdS quantum dots (QDs) with a high cytocompatibility and a tunable optical property based on alkaline post-treatment of Cd−GSH coordination polymers (CPs). Cd−GSH CPs are synthesized with the coordination reaction of Cd^{2+} with GSH at different pH values, and the CdS QDs are then formed by adding NaOH to the aqueous dispersion of the Cd−GSH CPs to break the coordination interaction between Cd^{2+} and GSH with the release of sulfur. The particle size and optical property of the as-formed CdS QDs are found to be easily tailored by simply adjusting the starting pH values of GSH solutions used for the formation of Cd−GSH CPs, in which the wavelengths of trap-state emission of the QDs red-shift with an increase in the sizes of the QDs that is caused by an increase in the starting pH values of GSH solutions. In addition, the use of GSH as the capping reagent eventually endows the as-formed CdS QDs with enhanced water solubility and good cytocompatibility, as demonstrated with HeLa cells. The method demonstrated here is advantageous in that the cadmium precursor and the sulfur source are nontoxic and easily available, and the size, optical properties, water solubility, and cytocompatibilty of the as-formed CdS QDs are simply achieved and experimentally regulated. This study offers a new and green synthetic route to water-soluble and cytocompatible CdS QDs with tunable optical properties.

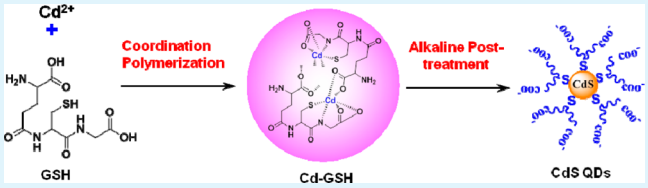

KEYWORDS: *CdS quantum dots, coordination polymers, green synthesis, glutathione, water solubility, cytocompatibility*

1. INTRODUCTION

Luminescent semiconductor nanocrystals, also known as quantum dots (QDs), have attracted intensive attention because of their excellent physicochemical properties, such as the quantum effect, luminosity, chemical processability,[1−3] and striking applications in various fields such as biological labeling, biosensing, electronics, optoelectronics, and solar cells.[4−12] As one of the most important group II−VI semiconductor nanocrystals, CdS has a direct band gap of 2.4 eV at room temperature[13] and has been extensively studied.[14−17] To date, a variety of synthetic approaches have been reported for CdS QDs, including an organometallic precursor-based hot injection route, thermolysis of a single-source precursor, solvothermal or hydrothermal synthesis, and a colloidal micellar method.[18−29] Although these methods have been demonstrated to be very useful for CdS QD synthesis, some of them require expensive and toxic materials, complicated procedures, and additional energy (such as heating, microwave, ultrasonication, and a mechanical alloying process) to promote synthesis. Furthermore, the CdS QDs synthesized with these methods are generally hydrophobic because of the uses of organic capping agents, which veritably endow the as-synthesized QDs with poor water solubility and less biocompatibility. These properties unfortunately invalidate the applications of the CdS QDs in biological studies such as biological labeling, biosensing, and drug delivery[30] because the water solubility and the biocompatibility of QDs have been reported to depend also on the surface molecules of QDs, not solely on their inherent toxic chemical composition.[31,32] As a consequence, it is imperative to develop a simple and environmentally friendly synthetic method for water-soluble CdS QDs with adequate hydrophilic and biocompatible surface capping agents to promote effectively the biological applications of CdS QDs.

Recently, two excellent strategies have been reported for the synthesis of water-soluble CdS QDs. One is based on either the exchange of the ligand with the hydrophobic QDs or in situ growth of a hydrophilic shell on the presynthesized QDs. The other is direct aqueous synthesis via arrested precipitation with phosphates, thiols, or hydrophilic polymers as the capping agents.[17,18,33−39] The former method is somewhat technically complicated requiring multiple experimental procedures such as the first preparation of the hydrophobic QDs and then ligand exchange or the growth of shell with some different precursors. The latter employs additional sulfur sources and the capping

Received: March 26, 2013
Accepted: May 13, 2013
Published: May 13, 2013

Scheme 1. (A) Illustration of the Formation of GSH-Capped CdS QDs by Alkaline Post-Treatment of Cd(II)−GSH Coordination Polymers[a] and (B) Different Modes of Coordination between Cd^{2+} and GSH in Cd−GSH CPs Formed at Different Starting pH Values of GSH Solutions (i.e., 7.0, 9.0, and 11.3)

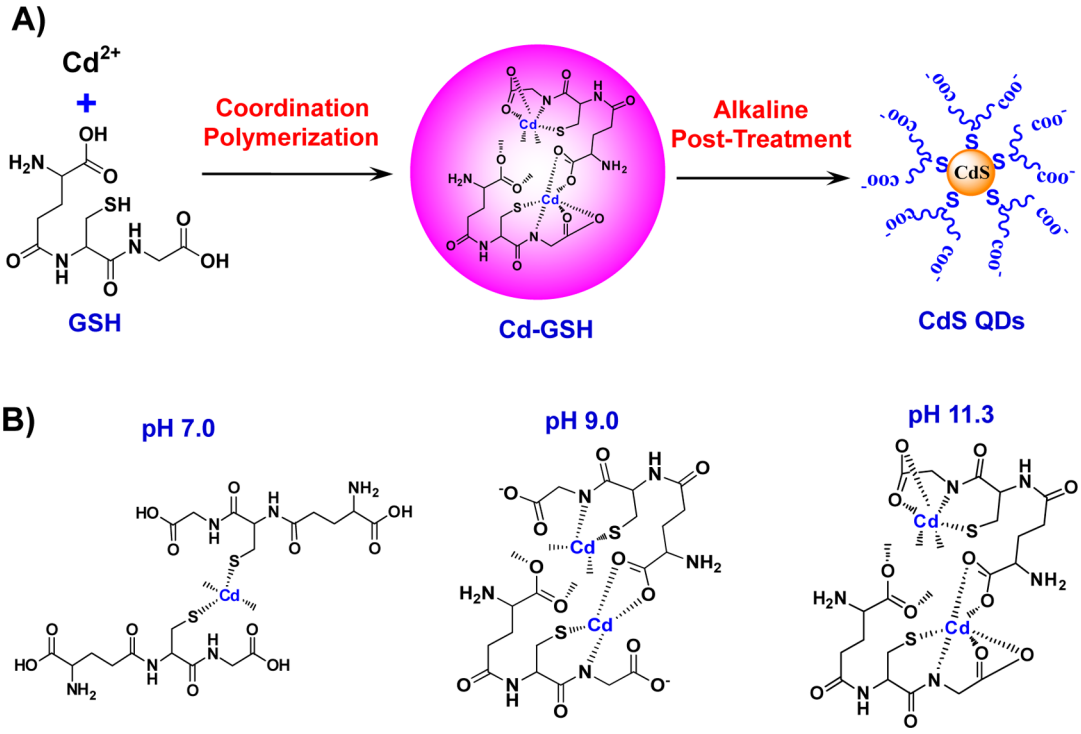

[a]The coordination between Cd^{2+} and GSH in Cd−GSH CPs forms in a GSH solution with a starting pH of 11.3.

agents and sometimes requires additional energy such as heating to promote the synthesis.

In this study, we demonstrate a novel method for green synthesis of CdS QDs with good water solubility and relatively high cytocompatibility through alkaline post-treatment of Cd(II)−glutathione (Cd−GSH) coordination polymers (CPs). As a fascinating family of porous hybrid materials built by self-assembling metal ions or metal ion clusters and polydentate organic bridging ligands,[40,41] CPs hold great promise for numerous attractive applications and have drawn a growing amount of attention from various research and industrial fields.[42−46] Recent efforts have revealed that post-treatment of CPs could offer a new paradigm for the fabrication of functional metal oxides and other kinds of nanostructures with size and morphology tailorability.[47−49]

In our synthetic approach, Cd−GSH CPs are formed with $CdCl_2$ as the cadmium precursor and GSH as both the sulfur sources and the capping agent, and the reactions are simply performed by adding $CdCl_2$ to a GSH solution at room temperature. The water-soluble GSH-capped CdS QDs are then formed simply by post-treating the as-synthesized QDs with alkaline media (Scheme 1A). The method demonstrated here is advantageous in the following aspects. (1) Unlike the conventional organometallic precursor-based hot injection synthetic methods, in which $Cd(CH_3)_2$ has been used as the cadmium precursor, nontoxic and less expensive cadmium chloride is used here. It is known that $Cd(CH_3)_2$ is highly toxic, pyrophoric, expensive, unstable at room temperature, and explosive at elevated temperatures because of the release of a large amount of gas.[50] (2) The frequently used sulfur sources in the existing methods employed for CdS QD synthesis include H_2S, thiourea, and other organic sulfides. These chemicals are more toxic and less environmentally friendly than the glutathione used in this study. (3) Different from the existing methods for CdS QD synthesis, the strategy demonstrated here does not require additional reagents, energy, or organic solvents. This property essentially makes our synthetic strategy more environmentally benign and experimentally simple. (4) The optical properties of the as-formed GSH-capped CdS QDs are easily tailored by simply adjusting the starting pH values of GSH solutions employed for the formation of Cd−GSH CPs. (5) Because this study utilizes water-soluble and biocompatible GSH as the capping agent for the synthesis of CdS QDs, the as-formed QDs possess good water solubility and high cytocompatibility, which are particularly attractive for biological applications.

2. EXPERIMENTAL SECTION

2.1. Chemicals. Cadmium chloride ($CdCl_2{\cdot}2.5H_2O$), glutathione (GSH), sodium hydroxide, and 2-propanol were all commercially available and used as received. GSH solutions with different starting pH values adjusted with a NaOH solution were freshly prepared before being used. Aqueous solutions were prepared with Milli-Q water (Millipore, 18.2 MΩ cm).

2.2. Synthesis of Cd−GSH Coordination Polymers and GSH-Capped CdS QDs. Cd−GSH CPs were synthesized through the coordination interaction between Cd^{2+} and GSH, in which Cd^{2+} is bound to the sulfhydryl group, the peptide linkage between the cysteinyl and glycyl residuals, and the carboxylic group of GSH. For the synthesis of Cd−GSH CPs, aqueous solutions of 10 mM GSH with different starting pH values (i.e., 7.0, 9.0, and 11.3) were first prepared. The same volumes of aqueous solutions of $CdCl_2{\cdot}2.5H_2O$ (10 mM) were mixed with the aqueous solutions of GSH with different starting pH values under magnetic stirring at room temperature, and the resulting precipitates (i.e., Cd−GSH CPs) were centrifuged, washed with water several times, and finally

redispersed in water for subsequent use. The GSH-capped CdS QDs (i.e., GSH−CdS QDs) were prepared through alkaline post-treatment of the as-formed Cd−GSH CPs by adding a NaOH solution to the aqueous dispersion of Cd−GSH CPs. In a typical experiment, a certain volume of a NaOH solution (10 mM) was added to the aqueous dispersion of Cd−GSH CPs, and the mixtures were kept at room temperature for 2 or 3 days. After that, 2-propanol was added to each mixture to form the precipitates. The formed precipitates (i.e., GSH−CdS QDs) were centrifuged, washed, and redispersed in water. Excess salt was removed by repeating the procedures mentioned above several times, and the purified QDs were dried at room temperature under vacuum.

Scanning electron microscopy (SEM) was performed on S-4300 and S-4800 instruments (Hitachi, Tokyo, Japan), and energy-dispersive X-ray (EDX) analysis was performed on an EDAX detector on the scanning electron microscope. Transmission electron microscopy (TEM) was performed on a JEOL JEM-2011 instrument (100 kV). Fourier transfer infrared (FTIR) spectra (KBr pellet) were collected on a Tensor-27 FTIR spectrometer (Bruker). UV−vis spectra were recorded at room temperature on a TU-1900 spectrometer. Fluorescence spectroscopy was conducted with an F-4600 fluorescence spectrophotometer (Hitachi). X-ray powder diffraction (XRD) was conducted using a Japan Rigaku D/max 2500 X-ray diffractometer with Cu Kα radiation (18 kW).

2.3. Cytotoxicity Assay. The HeLa line was supplied by Peking Union Medical College Hospital. HeLa cells were grown in Dulbecco's modified Eagle's medium (DMEM) supplemented with 10% FBS (fetal bovine serum) at 37 °C and 5% CO_2. The cytotoxicity of GSH−CdS QDs toward the HeLa cell lines was measured by a Cell Counting Kit-8 (CCK-8) assay. Before being incubated at 37 °C under a 5% CO_2 atmosphere for 12 and 24 h, HeLa cells growing in log phase were seeded into a 96-well cell culture plate at a density of 1×10^4 cells/well. The GSH−CdS QDs (100 μL/well) at concentrations of 400 μg/3 mL, 200 μg/3 mL, 100 μg/3 mL, 50 μg/3 mL, and 25 μg/3 mL were added to the wells for the experimental groups, and DMEM (100 μL/well) was added to the control group. The cells were incubated at 37 °C under a 5% CO_2 atmosphere for 12 and 24 h and washed with a phosphate-buffered solution (PBS) twice. The cells in the 96-well assay plate were added to a CCK-8/DMEM solution and incubated for an additional 2 h under the same conditions. An enzyme-linked immunosorbent assay (ELISA) reader (infinite M20, Tecan) was used to measure the OD_{450} (absorbance value) of each well referenced at 650 nm. The viability of cell growth was estimated as follows: viability (%) = [(mean absorbance value of the experimental group)/(mean absorbance value of the control group)] × 100.[51]

2.4. Cellular Uptake. The GSH−CdS QDs were dispersed into water to yield a final concentration of 10 mg/3 mL. Before being rinsed with PBS, HeLa cells were incubated solely with PBS (0.01 M, pH 7.4) containing GSH−CdS QDs (final concentration of 100 μg/3 mL) for 30 min at 37 °C under a 5% CO_2 atmosphere. Then, the fluorescent imaging of GSH−CdS QDs in HeLa cells was conducted on an Olympus FV1000 laser scanning confocal microscope and a 100× oil-immersion objective lens. A semiconductor laser was used for excitation of the HeLa cells incubated with GSH−CdS QDs at 405 nm. Emission was collected at 420−520 nm for the HeLa cells incubated solely with or without GSH−CdS QDs. The cellular uptake of GSH−CdS QDs was assessed by means of flow cytometry (CaAn ADP9). HeLa cells were incubated in serum free medium with or without GSH−CdS QDs (100 μg/3 mL) for 4 h at 37 °C under a 5% CO_2 atmosphere. The cells were harvested, rinsed in PBS, resuspended, and measured by flow cytometry.

3. RESULTS AND DISCUSSION

3.1. Formation of Cd−GSH CPs. Figure 1 displays the FTIR spectrum of the precipitates formed by adding $CdCl_2$ to a GSH solution with a starting pH of 11.3 (blue curve). For comparison, the spectrum of GSH was also given (black curve). For GSH, peaks at 2525, 3125 and 3027, 1600 and 1713, and 1537 cm^{-1} were assigned to the S−H stretching band (ν_{S-H}),

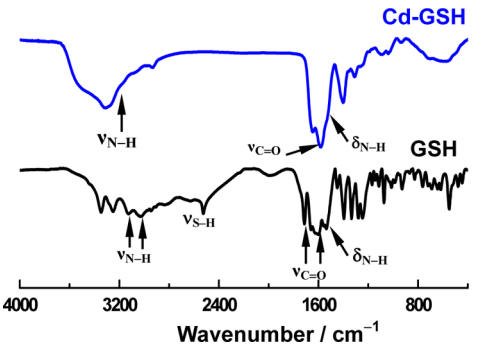

Figure 1. FTIR spectra of GSH (black) and Cd−GSH CPs (blue). Cd−GSH CPs were formed by addition of $CdCl_2$ to a GSH solution with a starting pH of 11.3. The y axis is transmittance.

the N−H (NH_3^+) stretching band (ν_{N-H}), the C═O stretching band of the carboxylic group ($\nu_{C=O}$), and the strong absorption peak of N−H deformation of the amide bond (δ_{N-H}), respectively.[52] After the addition of $CdCl_2$ to a GSH solution to form the precipitate, the characteristic peak of the S−H stretching disappears, the peaks of ν_{N-H} and δ_{N-H} shift to 3087 and 1578 cm^{-1}, respectively, and the peak of $\nu_{C=O}$ becomes relatively broad. These phenomena suggest the formation of Cd−GSH CPs through the coordination interaction between Cd^{2+} and GSH, in which Cd^{2+} is bound to the sulfhydryl group, the peptide linkage between the cysteinyl and glycyl residuals, and the carboxylic group of GSH. The presence of C, N, S, and Cd in the energy-dispersive X-ray (EDX) spectrum (Figure S1D of the Supporting Information) further confirms the formation of the Cd−GSH CPs, in which C, N, and S elements were ascribed to the presence of GSH. The peaks of Si and Ca arise from the glass substrate. Additionally, the featureless diffraction peaks indicate that the as-formed Cd−GSH CPs are amorphous and not crystalline (data not shown), which suggests that the Cd−GSH CPs are one kind of infinite coordination polymer (ICPs).[41] Note that, under these conditions, $Cd(OH)_2$ was not formed mainly because the coordination interaction between Cd^{2+} and GSH was stronger than that between Cd^{2+} and OH^-.[53]

SEM images (Figure S1A−C of the Supporting Information) reveal that the resulting Cd−GSH CPs formed in the GSH solutions with different starting pH values of 7.0, 9.0, and 11.3 were all spherical colloids with relatively smooth surfaces. More interestingly, we found that the size of the as-formed Cd−GSH CPs was dependent on the starting pH values of GSH solutions; with an increase in the starting pH values, the size of the CPs becomes smaller. For instance, the sizes of the Cd−GSH CPs prepared at pH 7.0, 9.0, and 11.3 were ~1266 ± 285, ~474 ± 119, and ~42 ± 10 nm, respectively. We also found that the Cd−GSH CPs prepared at pH 11.3 were easily aggregated (Figure S1C of the Supporting Information), which was presumably ascribed to the fast growth rate at such a pH value. Early efforts have demonstrated that the size and morphology of CPs could be manipulated by controlling the experimental conditions, including the reaction time, reaction temperature, reactant concentration or molar ratio, and the addition of additives,[54,55] of which the addition of acids or bases was found to be able to tune the size and morphology of the as-formed CPs because such a process modulated the deprotonation rate of organic linkers or blocked the growth of nuclei for a specific direction.[55] GSH used in this study is a tripeptide with several potential coordination sites such as the sulfhydryl

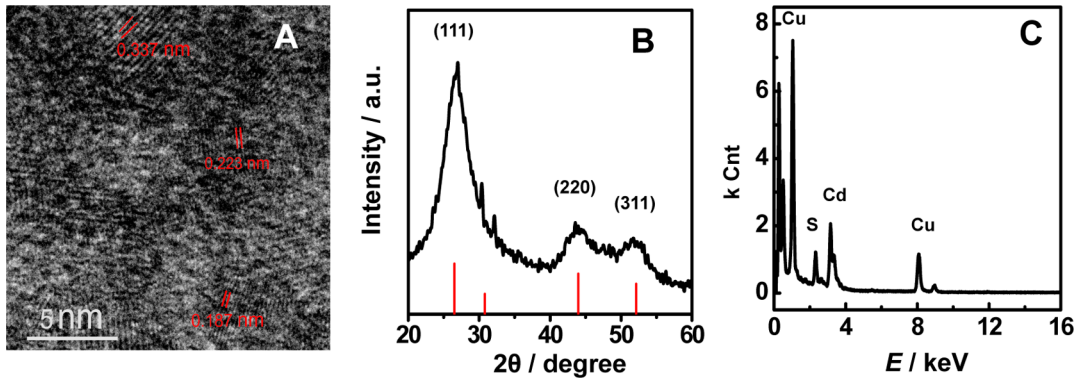

Figure 2. (A) HRTEM image of GSH−CdS QDs obtained by alkaline post-treatment of Cd−GSH CPs formed by addition of $CdCl_2$ to a GSH solution at a starting pH of 11.3. (B) XRD pattern (black curve, synthesized GSH−CdS QDs; red curve, simulated pattern). (C) EDX spectrum of GSH−CdS QDs formed by alkaline post-treatment of Cd−GSH CPs prepared at a starting pH of 11.3. The peaks of Cu arise from the substrate.

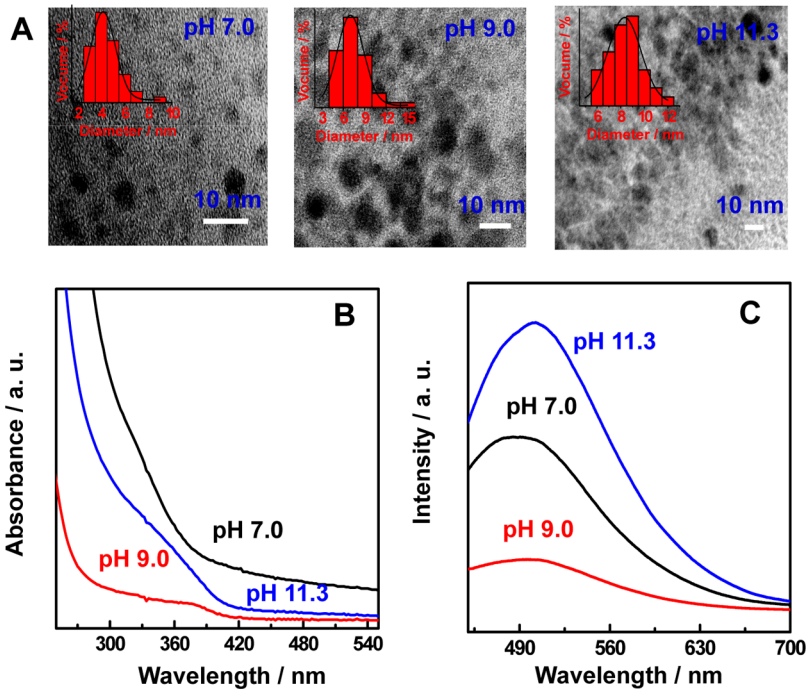

Figure 3. (A) TEM images of GSH−CdS QDs obtained by alkaline post-treatment of Cd−GSH CPs formed by addition of $CdCl_2$ to a GSH solution at starting pH values of 7.0, 9.0, and 11.3 (as indicated). The insets show particle size distributions of the corresponding GSH−CdS QDs. (B) UV−vis absorption and (C) fluorescence spectra of GSH−CdS QDs formed at different starting pH values for the reaction system (λ_{ex} = 365 nm).

group, carboxyl group, and amide group of the residuals. The observed dependence of the size of the Cd−GSH CPs on the starting pH values of GSH solutions (Figure S1A−C of the Supporting Information) could be understood by the pH-controlled deprotonation rate of GSH. Specifically, the different pH-controlled deprotonation rates of GSH could result in the exposure of different coordination sites, which eventually brings about different modes of coordination between Cd^{2+} and GSH at different starting pH values[53] (Scheme 1B). One can see that, at low pH values, GSH is a linear molecule and keeps its original state even if it is coordinated with Cd^{2+}. That is, the long carbon chain of the GSH molecule still extends freely, and its side chain keeps dangling. At high pH values, the carbon chain has a subtle twist to make it easy for GSH to coordinate with Cd^{2+} at different coordination sites, forming the small Cd−GSH CPs (Figure S1C of the Supporting Information).

3.2. Formation of GSH−CdS QDs. As mentioned above, GSH-capped CdS QDs (abbreviated as GSH−CdS QDs hereafter) were synthesized by post-treatment of the as-formed Cd−GSH CPs by adding an equal volume of a NaOH (10 mM) solution to the aqueous dispersion of the Cd−GSH CPs and allowing the mixture to stand for 2 or 3 days at room temperature. As displayed in the high-resolution TEM (HRTEM) image (Figure 2A), the GSH−CdS QDs prepared by NaOH post-treatment of the Cd−GSH CPs synthesized at a starting pH of 11.3 exhibit good crystallinity. The lattice fringes with interplanar spacings of 0.337, 0.223, and 0.187 nm indicate that the QDs were ascribed to the (111), (220), and (311) planes, respectively, of the cubic zinc blende structure of CdS. The XRD pattern (Figure 2B) with diffraction peaks (111), (220), and (311) again shows that the as-prepared sample was indexed to cubic zinc blende CdS.[21] For the XRD patterns, the relatively broad diffraction peaks here were attributed to the

small sizes of the as-synthesized CdS nanocrystals,[18] which was consistent with the size distribution demonstrated in the TEM image shown below (Figure 3A). The presence of S and Cd elements in the EDX spectrum (Figure 2C) further confirms the formation of GSH−CdS QDs, in which the atomic ratio of S to Cd was estimated to be 1.37:1.00. This ratio, to some extent, suggests that some of GSH molecules act as the capping agents because the atomic ratio of S to Cd is higher than the theoretical one (1:1). These results demonstrate that alkaline post-treatment of coordination polymers can be exploited for the facile synthesis of CdS QDs, which is greener and simpler than the traditional synthetic approaches (Table S1 of the Supporting Information).

More remarkably, the size of the CdS nanocrystals synthesized with our method could be simply tuned by adjusting the starting pH values of GSH solutions used for the synthesis of Cd−GSH CPs. As displayed in Figure 3A, the CdS nanocrystals prepared by NaOH post-treatment of the Cd−GSH CPs synthesized with the starting pH values of GSH solutions (i.e., pH 7.0, 9.0, and 11.3) were spherical in shape with average sizes of 3.97 ± 1.22, 7.37 ± 2.21, and 8.38 ± 1.49 nm, respectively. These results demonstrate that the size of the CdS nanocrystals prepared with our strategy was simply tunable, which was very advantageous compared to the existing methods.

3.3. Tunable Optical Properties of GSH−CdS QDs. In addition to the uses of the green cadmium precursor and sulfur source and the easily tunable size of the GSH−CdS QDs synthesized with our method, we found that the optical properties of the QDs synthesized in this study strongly depend on their size, providing the opportunity to tune the optical properties of the QDs simply by adjusting the starting pH values of GSH solutions. The GSH−CdS QDs formed at different starting pH values of GSH solutions were investigated by UV−vis absorption (Figure 3B) and fluorescence (Figure 3C) spectroscopy. As one can see in Figure 3B, the UV−vis absorption onsets were nearly 390, 401, and 410 nm for the GSH−CdS QDs formed in the reaction systems with starting pH values of 7.0, 9.0, and 11.3, respectively. Because the typical band gap of bulky zinc blende CdS is 2.4 eV, which corresponds to an absorption onset of 515 nm,[56] the dramatic starting pH-induced blue shift of the absorption onset wavelength presumably suggests the quantum confinement effect when the semiconductor particle is smaller than or comparable to the Bohr excitation radius (6 nm).[26] Additionally, the absorption onsets of the synthesized GSH−CdS QDs shift to longer wavelengths with an increase in the starting pH values, indicating the faster growth rate during the process of QD formation and thus the increase in the size of the QDs with an increase in the starting pH values, as observed in Figure 3A.

According to the literature,[20,35,52] the difference in reaction activities of the precursors could cause the difference in the growth rate of the QDs. In this study, the difference in reaction activities of the precursors was mainly related to the different stabilities against alkaline post-treatment of the Cd−GSH CPs because of the different modes of coordination of GSH with Cd^{2+} at different starting pH values. Among the Cd−GSH CPs synthesized with different starting pH values, those synthesized with low starting pH values were more stable; thus, their growth rate was much slower, generating the small QDs, and vice versa.

The luminescence properties of the prepared GSH−CdS QDs were investigated by fluorescence measurements (Figure 3C). It should be mentioned that the prepared Cd−GSH CPs were nonemissive under 365 nm excitation (data not shown), whereas the GSH−CdS QDs synthesized by alkaline post-treatment of the Cd−GSH CPs were emissive because of the quantum confinement effect. Furthermore, we have also compared the luminescence properties of the GSH−CdS QDs formed at different starting pH values. As shown in Figure 3C, relatively broad emission peaks were observed at ∼485, ∼495, and ∼502 nm for the QDs synthesized in the reaction systems with the starting pH values of 7.0, 9.0, and 11.3, respectively. The cover range of the fluorescence spectra is 485−502 nm, with starting pH values from 7.0 to 11.3. The quantum yields of the GSH−CdS QDs with starting pH values of 7.0, 9.0, and 11.3 were calculated to be 1, 8, and 4%, respectively, with 0.5 M quinine sulfate in sulfuric acid as the reference. The emission peaks correspond to trap-state emission involving the recombination of electrons with holes at the surface defects.[57] The single-peak trap-state emission band indicates one set of trap states.[26,38] Because the radius of S^{2-} is smaller than that of Cd^{2+},[26] sulfur vacancy more easily exists in the CdS materials. Therefore, the trap-state emission in our method may be attributed to sulfur vacancy. We found that the emission wavelengths of the QDs show a red-shift tendency with an increase in the starting pH values. Previous studies have suggested that, along with the band edges, the energies of the trap states could also change with particle size, resulting in particle size-dependent trap-state emission.[34,38] From the luminescence properties of the GSH−CdS QDs formed at different starting pH values, we may draw a conclusion that the QDs become larger with an increase in the starting pH values, which was consistent with the TEM results (Figure 3A). Moreover, the intensities of trap-state emission of the QDs prepared at the different starting pH values of the reaction systems were quite different. We speculated that the different coordination modes may generate Cd−GSH CPs with different surface states. Therefore, after alkaline post-treatment, the formed GSH−CdS QDs have different surface defect states. The different trap-state emission of CdS QDs could thus be understood by the different quantity of sulfur vacancy located at the surface of the QDs.

3.4. Enhanced Water Solubility and Good Cytocompatibility of GSH−CdS QDs. The synthesized GSH−CdS QDs were water-soluble (Figure 4, inset) mainly because of the

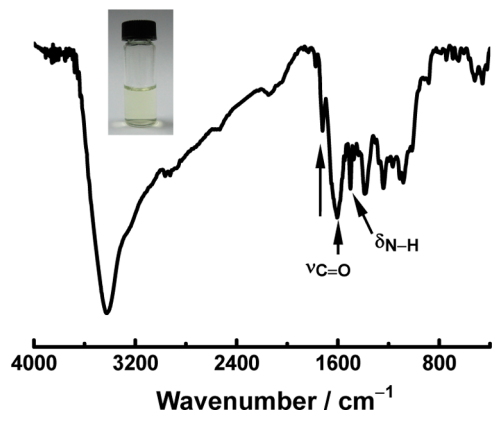

Figure 4. FTIR spectra of GSH−CdS QDs obtained by alkaline post-treatment of Cd−GSH CPs formed in the GSH solutions at a starting pH of 11.3. The *y* axis is transmittance. The inset is a photograph of the aqueous dispersion of GSH−CdS QDs.

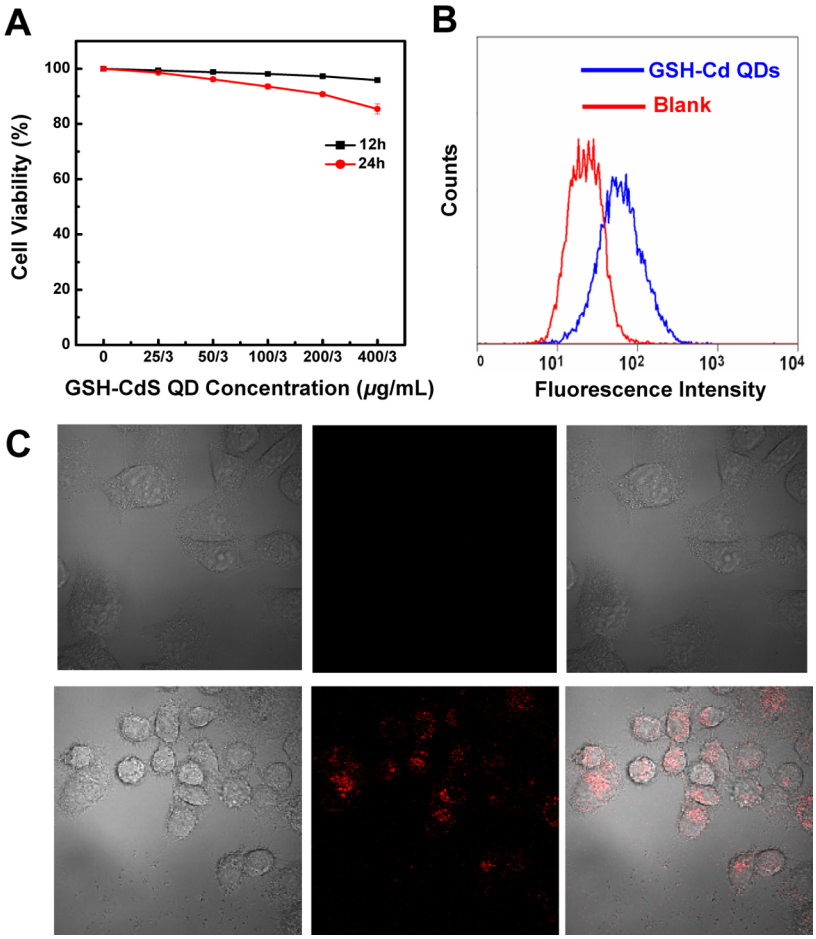

Figure 5. (A) Cytotoxicity of GSH−CdS QDs at different concentrations and incubation times with HeLa cells. (B) Flow cytometry assay to evaluate the uptake of HeLa cells in an aqueous solution of GSH−CdS QDs (10 μg/3 mL). (C) Confocal luminescent images of HeLa cells (top) incubated solely with the PBS (0.01 M, pH 7.4) and (bottom) incubated with the PBS (0.01 M, pH 7.4) of GSH−CdS QDs (final concentration of 100 μg/3 mL) for 30 min at 37 °C under a 5% CO_2 atmosphere (λ_{ex} = 405 nm; λ_{em} = 420−520 nm).

presence of GSH as the capping agents. To verify this hypothesis, FTIR spectrometry was conducted to investigate the ultimate surface capping structure of the GSH−CdS QDs (Figure 4). The GSH−CdS QDs show two relatively strong peaks located at 1721 cm^{-1} for the C═O stretching bands of the carboxylic group and a weak peak located at 1546 cm^{-1} for the N−H (δ_{N-H}) deformation of the amide bond.[52] Additionally, the disappearance of the S−H stretching bands (ν_{S-H}) at 2525 cm^{-1} is likely the result of the formation of a covalent bond between the thiol and Cd atom at the CdS QD surface, suggesting the oxidation of cysteine residues.[58] By comparing with the FTIR spectrum of GSH (Figure 1, black curve), we found that the carboxylic group of GSH remains on the surface of the QDs, which could be used as the capping agent for the QDs. The presence of a hydrophilic group of carboxylate on the surface of GSH−CdS QDs is responsible for the water solubility of the GSH−CdS QDs synthesized by our method. Such a property will largely allow the GSH−CdS QDs to be widely used in research fields such as biological labeling, biosensing, drug delivery, etc.

The as-synthesized GSH−CdS QDs also show good cytocompatibility, which eventually makes them very promising for biological applications such as cell imaging. The cytotoxicity of QDs on cultured cells was thus evaluated; HeLa cells were incubated for 12 and 24 h after being treated with the GSH−CdS QDs, and then a CCK-8 assay was performed. As shown in Figure 5A, no significant differences in the proliferation of the cells were observed in the absence or presence of CdS QDs. In the presence of CdS QDs, at the same concentration, the cellular viabilities were estimated to be greater than 85% after incubation for 12 and 24 h, and an only minimal change in cell viability was observed for cells after treatment with the GSH−CdS QDs at different concentrations (25 μg/3 mL, 50 μg/3 mL, 100 μg/3 mL, 200 μg/3 mL, and 400 μg/3 mL), suggesting the GSH−CdS QDs have a low cytotoxicity on the cells.

Because of the excellent reproducibility, a high degree of statistical precision due to the large number of cells measured, the quantitative nature of the analysis, and the high speed, the flow cytometry assay has been used as the best way to monitor the enrichment process.[59] Here, we applied such a method to evaluate cellular uptake of a GSH−CdS QD aqueous solution (10 μg/3 mL) under different conditions. Figure 5B shows that the increase in the fluorescence intensity on HeLa cells was observed in flow cytometry analysis. This result indicates that a significant number of HeLa cells have taken up the GSH−CdS QDs and successfully been labeled. Fluorescence imaging of living HeLa cells using GSH−CdS QDs was conducted via confocal fluorescence microscopy. The confocal fluorescence microscopy images of living HeLa cells incubated with GSH−CdS QDs with 405 nm excitation are shown in Figure 5C. The intensity profile of GSH−CdS QD-treated HeLa cells reveals

dx.doi.org/10.1021/am401082n | ACS Appl. Mater. Interfaces 2013, 5, 5239−5246

that most of QDs were distributed in the cytoplasm surrounding the nuclei, suggesting that GSH−CdS QDs were taken up by the cells and acted as a fluorescence imaging agent for cells without requiring prior membrane permeabilization.[51] This demonstrates that GSH−CdS QDs are good fluorescent tags and could be potentially used in biolabeling, cell imaging, and so forth.

4. CONCLUSIONS

In summary, we have demonstrated a novel and facile aqueous route to the synthesis of water-soluble GSH-capped CdS QDs at room temperature by alkaline post-treatment of Cd−GSH coordination polymers, in which the cadmium precursor and the sulfur source are nontoxic and easily available and no additional substances or energy is necessitated. With a change in the starting pH values of GSH solutions, the particle size of the formed GSH−CdS QDs can be easily tuned, resulting in the tunable emission wavelengths of the CdS QDs due to the particle size-dependent trap-state emission of QDs. Moreover, the use of GSH as the capping agents endows the as-formed CdS QDs with high water solubility and cytocompatibility. The aqueous synthetic approach demonstrated here is very simple, mild, and environmentally friendly, and the size, optical properties, water solubility, and cytocompatibilty of the as-formed CdS QDs could be simply achieved and experimentally regulated. These excellent properties of the as-synthesized QDs substantially allow them to be particularly attractive in fields such as biological labeling, biosensing, and drug delivery. Additionally, the strategy demonstrated here for the formation of water-soluble CdS QDs through alkaline post-treatment of Cd−GSH coordination polymers may open a new synthetic avenue for the post-treatment of coordination polymers to functional materials with excellent properties.

■ ASSOCIATED CONTENT

Supporting Information

SEM images of Cd−GSH CPs formed by addition of $CdCl_2$ to GSH solutions with different starting pH values of 7.0, 9.0, and 11.3; mechanism of formation of GSH−CdS QDs; elucidation of the low cytotoxicity of CdS QDs; and a table of comparison of the synthetic conditions for CdS QDs employed in the existing methods and our method. This material is available free of charge via the Internet at http://pubs.acs.org.

■ AUTHOR INFORMATION

Corresponding Author

*E-mail: lqmao@iccas.ac.cn (L.M.) or yanglf@iccas.ac.cn (L.Y.). Fax: +86-10-62559373.

Notes

The authors declare no competing financial interest.

■ ACKNOWLEDGMENTS

We acknowledge financial support from the National Natural Science Foundation of China (Grants 20935005, 21127901, 91213305, and 21210007 to L.M. and 21175141 for L.Y.), the National Basic Research Program of China (973 program, 2010CB33502, 2013CB933704), and the Chinese Academy of Sciences (KJCX2-YW-W25).

■ REFERENCES

(1) Wang, Y.; Herron, N. *J. Phys. Chem.* **1991**, *95*, 525−532.
(2) Pradhan, N.; Sarma, D. D. *J. Phys. Chem. Lett.* **2011**, *2*, 2818−2826.
(3) Akamatsu, K.; Tsuruoka, T.; Nawafune, H. *J. Am. Chem. Soc.* **2005**, *127*, 1634−1635.
(4) Hildebrandt, N. *ACS Nano* **2011**, *5*, 5286−5290.
(5) Wang, Q.; Xu, Y.; Zhao, X.; Chang, Y.; Liu, Y.; Jiang, L.; Sharma, J.; Seo, D.; Yan, H. *J. Am. Chem. Soc.* **2007**, *129*, 6380−6381.
(6) Sharma, J.; Ke, Y.; Lin, C.; Chhabra, R.; Wang, Q.; Nangreave, J.; Liu, Y.; Yan, H. *Angew. Chem., Int. Ed.* **2008**, *47*, 5157−5159.
(7) Nann, T.; Skinner, W. M. *ACS Nano* **2011**, *5*, 5291−5295.
(8) Wang, Q.; Iancu, N.; Seo, D. *Chem. Mater.* **2005**, *17*, 4762−4764.
(9) Huynh, W. U.; Dittmer, J. J.; Alivisatos, A. P. *Science* **2002**, *295*, 2425−2427.
(10) Wu, P.; He, Y.; Wang, H.; Yan, X. *Anal. Chem.* **2010**, *82*, 1427−1433.
(11) Luo, M.; Liu, Y.; Hu, J.; Liu, H.; Li, J. *ACS Appl. Mater. Interfaces* **2012**, *4*, 1813−1821.
(12) He, H.; Feng, M.; Hu, J.; Chen, C.; Wang, J.; Wang, X.; Xu, H.; Lu, J. R. *ACS Appl. Mater. Interfaces* **2012**, *4*, 6362−6370.
(13) Shen, G. Z.; Cho, J. H.; Yoo, J. K.; Yi, G. C.; Lee, C. J. *J. Phys. Chem. B* **2005**, *109*, 9294−9298.
(14) Duxin, N.; Liu, F.; Vali, H.; Eisenberg, A. *J. Am. Chem. Soc.* **2005**, *127*, 10063−10069.
(15) Ahmad, A.; Mukherjee, P.; Mandal, D.; Senapati, S.; Khan, M. I.; Kumar, R.; Sastry, M. *J. Am. Chem. Soc.* **2002**, *124*, 12108−12109.
(16) Habas, S. E.; Yang, P.; Mokari, T. *J. Am. Chem. Soc.* **2008**, *130*, 3294−3295.
(17) Chen, Y.; Rosenzweig, Z. *Anal. Chem.* **2002**, *74*, 5132−5138.
(18) Zhuang, Z.; Lu, X.; Peng, Q.; Li, Y. *J. Am. Chem. Soc.* **2010**, *132*, 1819−1821.
(19) Joo, J.; Na, H. B.; Yu, T.; Yu, J. H.; Kim, Y. W.; Wu, F.; Zhang, J. Z.; Hyeon, T. *J. Am. Chem. Soc.* **2003**, *125*, 11100−11105.
(20) Yu, W. W.; Peng, X. *Angew. Chem., Int. Ed.* **2002**, *41*, 2368−2371.
(21) Cao, C. Y.; Wang, J. *J. Am. Chem. Soc.* **2004**, *126*, 14336−14337.
(22) Nair, S. P.; Scholes, G. D. *J. Mater. Chem.* **2006**, *16*, 467−473.
(23) Barrelet, C. J.; Wu, Y.; Bell, D. C.; Lieber, C. M. *J. Am. Chem. Soc.* **2003**, *125*, 11498−11499.
(24) Pradhan, N.; Efrima, S. *J. Am. Chem. Soc.* **2003**, *125*, 2050−2051.
(25) Zhang, X.; Zhao, Q.; Tian, Y.; Xie, Y. *Cryst. Growth Des.* **2004**, *4*, 355−359.
(26) Wang, X.; Feng, Z.; Fan, D.; Fan, F.; Li, C. *Cryst. Growth Des.* **2010**, *10*, 5312−5318.
(27) Wang, L.; Li, P.; Zhuang, J.; Bai, F.; Feng, J.; Yan, X.; Li, Y. *Angew. Chem., Int. Ed.* **2008**, *47*, 1054−1057.
(28) Gao, F.; Lu, Q.; Meng, X.; Komarneni, S. *J. Phys. Chem. C* **2008**, *112*, 13359−13365.
(29) Khomane, R. B.; Manna, A.; Mandale, A. B.; Kulkarni, B. D. *Langmuir* **2002**, *18*, 8237−8240.
(30) Larson, D. R.; Zipfel, W. R.; Williams, R. M.; Clark, S. W.; Bruchez, M. P.; Wise, F. W.; Webb, W. W. *Science* **2003**, *300*, 1434−1436.
(31) Tan, S. J.; Jana, N. R. S.; Patra, P. K.; Ying, J. Y. *Chem. Mater.* **2010**, *22*, 2239−2247.
(32) Hoshino, A.; Fujioka, K.; Oku, T.; Suga, M.; Sasaki, Y. F.; Ohta, T.; Yasuhara, M.; Suzuki, K.; Yamamoto, K. *Nano Lett.* **2004**, *4*, 2163−2169.
(33) Sapra, S.; Nanda, J.; Sarma, D. D.; El-Al, F. A.; Hodes, G. *Chem. Commun.* **2001**, *37*, 2188−2189.
(34) Li, H.; Shih, W. Y.; Shih, W. *Ind. Eng. Chem. Res.* **2007**, *46*, 2013−2019.
(35) Zou, L.; Fang, Z.; Gu, Z.; Zhong, X. *J. Lumin.* **2009**, *129*, 536−540.
(36) Barglik-Chory, C.; Buchold, D.; Muller, G. *Chem. Phys. Lett.* **2003**, *379*, 443−451.
(37) Gabellieri, E.; Cioni, P.; Balestreri, E.; Morelli, E. *Eur. Biophys. J.* **2011**, *40*, 1237−1245.
(38) Qi, L.; Colfen, H.; Antonietti, M. *Nano Lett.* **2001**, *1*, 61−65.

(39) Maheshwari, V.; Saraf, R. F. *Langmuir* **2006**, *22*, 8623−8626.
(40) Yaghi, O. M.; O'Keeffe, M.; Ockwig, N. W.; Chae, H. K.; Eddaoudi, M.; Kim, J. *Nature* **2003**, *423*, 705−714.
(41) Spokoyny, A. M.; Kim, D.; Sumrein, A.; Mirkin, C. A. *Chem. Soc. Rev.* **2009**, *38*, 1218−1227.
(42) Huang, P.; Mao, J.; Yang, L.; Yu, P.; Mao, L. *Chem.—Eur. J.* **2011**, *17*, 11390−11393.
(43) Park, K. H.; Jang, K.; Son, S. U.; Sweigart, D. A. *J. Am. Chem. Soc.* **2006**, *128*, 8740−8741.
(44) Nishiyabu, R.; Hashimoto, N.; Cho, T.; Watanabe, K.; Yasunaga, T.; Endo, A.; Kaneko, K.; Niidome, T.; Murata, M.; Adachi, C.; Katayama, Y.; Hashizume, M.; Kimizuka, N. *J. Am. Chem. Soc.* **2009**, *131*, 2151−2158.
(45) Yang, L.; Kinoshita, S.; Yamada, T.; Kanda, S.; Kitagawa, H.; Tokunaga, M.; Ishimoto, T.; Ogura, T.; Nagumo, R.; Miyamoto, A.; Koyama, M. *Angew. Chem., Int. Ed.* **2010**, *49*, 5348−5351.
(46) Gu, Z. Y.; Yang, C. X.; Chang, N.; Yan, X. P. *Acc. Chem. Res.* **2012**, *5*, 734−745.
(47) Jung, S.; Cho, W.; Lee, H. J.; Oh, M. *Angew. Chem., Int. Ed.* **2009**, *48*, 1459−1462.
(48) Park, J.; Lee, H. J.; Cho, W.; Jo, C.; Oh, M. *Adv. Mater.* **2011**, *23*, 3161−3164.
(49) Zhang, L.; Wang, L.; Guo, S.; Zhai, J. G.; Dong, S.; Wang, E. *Electrochem. Commun.* **2009**, *11*, 258−261.
(50) Peng, Z. A.; Peng, X. *J. Am. Chem. Soc.* **2001**, *123*, 183−184.
(51) Li, C.; Yu, M.; Sun, Y.; Wu, Y.; Huang, C.; Li, F. *J. Am. Chem. Soc.* **2011**, *133*, 11231−11239.
(52) Zhang, J.; Li, J.; Zhang, J.; Xie, R.; Yang, W. *J. Phys. Chem. C* **2010**, *114*, 11087−11091.
(53) Fuhr, B. J.; Rabenstein, D. L. *J. Am. Chem. Soc.* **1973**, *95*, 6944−6950.
(54) Jung, S.; Oh, M. *Angew. Chem., Int. Ed.* **2008**, *47*, 2049−2051.
(55) Cho, W.; Lee, H. J.; Oh, M. *J. Am. Chem. Soc.* **2008**, *130*, 16943−16946.
(56) Sone, E. D.; Stupp, S. I. *J. Am. Chem. Soc.* **2004**, *126*, 12756−12757.
(57) O'Sullivan, C.; Gunning, R. D.; Sanyal, A.; Barrett, C. A.; Geaney, H.; Laffir, F. R.; Ahmed, S.; Ryan, K. M. *J. Am. Chem. Soc.* **2009**, *131*, 12250−12257.
(58) Zhang, L.; Xu, C.; Li, B. *Microchim. Acta* **2009**, *166*, 61−68.
(59) Shangguan, D.; Meng, L.; Cao, Z. C.; Xiao, Z.; Fang, X.; Li, Y.; Cardona, D.; Witek, R. P.; Liu, C.; Tan, W. *Anal. Chem.* **2008**, *80*, 721−728.